Femtosecond Scattering Dynamics in Magnetic Semiconductor Spin Superlattices

J. F. Smyth, D. A. Tulchinsky, and D. D. Awschalom
Department of Physics, University of California, Santa Barbara, California 93106

N. Samarth
Department of Physics, The Pennsylvania State University, University Park, Pennsylvania 16802

H. Luo and J. K. Furdyna
Department of Physics, University of Notre Dame, Notre Dame, Indiana 46556
(Received 20 January 1993)

Spin-dependent dynamics of polarized carriers in a series of $Zn_{1-x}Mn_xSe/ZnSe$ superlattice structures are directly observed by time-resolved upconversion photoluminescence spectroscopy at low temperatures. Polarization measurements in small magnetic fields reveal spin-flip scattering of carriers confined within a magnetic quantum well. A marked change in the dynamics is observed with increasing field and subsequent spin superlattice formation. Exciton lifetimes and spin relaxation are seen to be strongly dependent on both the energy and *location* of spin states in the heterostructure.

PACS numbers: 71.35.+z, 75.50.Rr, 78.20.Ls, 78.47.+p

The dynamical behavior of excitons in quantum confined geometries has elicited substantial experimental and theoretical interest for several years, resulting in a detailed understanding of the energy relaxation process for excitons in semiconductor quantum wells [1]. By comparison, our knowledge of the *spin* relaxation process for excitons and carriers in quantum wells is still at a nascent stage and it is only in recent years that serious attention has been directed to the understanding of exciton spin dynamics in quantum well configurations [2–5]. A particularly attractive class of systems in which to address the connection between spin relaxation and quantum confinement is provided by quantum wells and superlattices containing diluted magnetic semiconductors (DMS). In this context, an important type of structure is the "spin superlattice" (SSL) in which alternating layers of a magnetic and a nonmagnetic semiconductor are chosen such that there is essentially no quantum confining potential in zero magnetic field [6–9]. The application of a magnetic field induces a spin-dependent confining potential that eventually leads to a spatial separation of the opposite spin states of the electron and hole wave functions [Fig. 1(a)]. Here we describe femtosecond polarization-resolved luminescence studies of SSL structures which reveal carrier spin scattering that is strongly dependent on the detected energy and applied magnetic field. In low fields, excitons are confined to the magnetic $Zn_{1-x}Mn_xSe$ quantum wells where spin-flip scattering is directly observed on time scales indicative of *sp-d* exchange interactions [2]. With increasing field the SSL forms and an extremely rapid spin relaxation of carriers localized in the nonmagnetic ZnSe layers occurs. Both regimes display dynamical behavior which is markedly different from that seen in traditional DMS structures [3] or expectations inferred from static measurements in SSL's with different strain and magnetic composition [8].

The experiments use a series of $Zn_{1-x}Mn_xSe/ZnSe$ multilayer structures that were previously established as "spin superlattices" using magneto-optical absorption spectroscopy [6]. Each structure consists of a ten period sequence of {100 Å ZnSe/100 Å $Zn_{1-x}Mn_xSe$} grown on (100) GaAs after a 1 μm ZnSe buffer. The Mn composition in the series ranges from $x=0.05$ to $x=0.09$. The $Zn_{1-x}Mn_xSe$ layers are coherently strained so that the in-plane lattice parameter matches that of the unstrained ZnSe layers, hence removing the heavy-hole–light-hole degeneracy *only* in the $Zn_{1-x}Mn_xSe$ layers. Taking into account the strain and bowing of the $Zn_{1-x}Mn_xSe$ band gap, there is a minimal (5 meV) band offset for both the valence (heavy hole) and conduction bands in zero applied magnetic field. Figure 1(a) shows that the carriers are spatially confined to the magnetic layers for $0 < B < B_{SSL}$, where $B_{SSL} \sim 0.5$ T is the field required to form the SSL. For $B > B_{SSL}$, the large Zeeman splitting of the $Zn_{1-x}Mn_xSe$ band edge overcomes the zero field offsets and results in the formation of a SSL in which the spin states of the electrons and holes are spatially and periodically separated. The details of the SSL transition are reported elsewhere [6]. In these studies the samples are positioned in a variable temperature magneto-optical cryostat at $T=4.2$ K and measured in the Faraday configuration. Symmetry considerations show that the luminescence in the presence of a magnetic field is either left- (σ^-) or right- (σ^+) circularly polarized with the helicity determined by the spin state of the radiating exciton. To resolve the two circular polarized components of the luminescence, and hence monitor the spin states of the excitons directly, a $\lambda/4$ wave plate is used followed by a linear polarizer.

Time-resolved photoluminescence spectroscopy is performed in these systems using sum-frequency upconversion techniques [10]. In this method, a laser pulse is used to excite the sample and a time-delayed probe pulse inter-

0031-9007/93/71(4)/601(4)$06.00

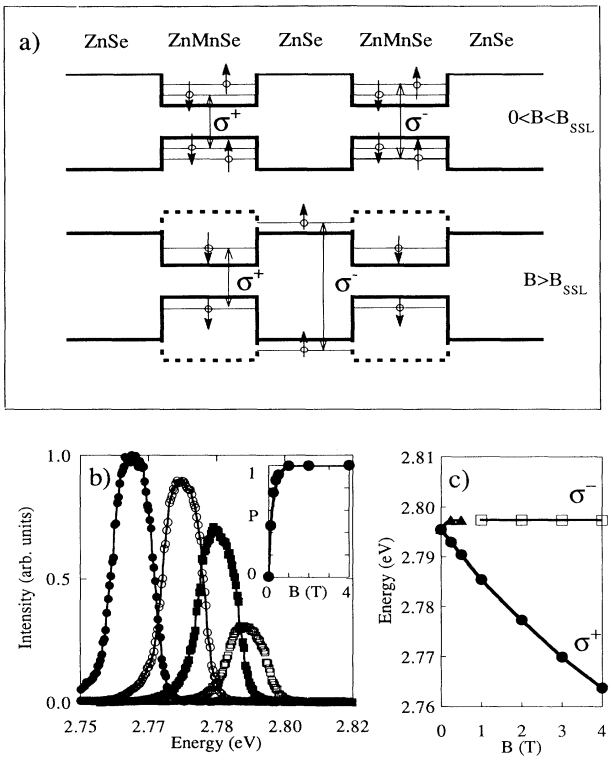

FIG. 1. (a) Schematic diagram showing the band offsets and energy levels of the spin states for the two field-dependent regimes. (b) Time-integrated σ^+ component of the PL from a $Zn_{0.91}Mn_{0.09}Se/ZnSe$ SSL [$B=\frac{1}{4}$ (□), 1 (■), 2 (○), 4 (●) T]. Inset: Field dependence of the time-integrated polarization. (c) Energy of the σ^+ and σ^- luminescence peak with applied magnetic field. Open squares represent PL from the ZnSe buffer layer.

rogates a time slice of the collected luminescence as the two pass coincidentally through a thin β-barium borate (BBO) nonlinear crystal. Sum-frequency photons are then generated for those luminescence wavelengths which, along with the probe beam, satisfy the phase-matching conditions of the crystal. In practice, "blue" femtosecond excitation pulses between 2.75 and 3.10 eV are generated by collinear, second harmonic generation in a thin BBO crystal using the transform limited infrared output of a mode-locked titanium sapphire laser. Sum-frequency photons are efficiently generated using a mixing scheme in which a portion of the infrared pulses are used to probe the collected luminescence with resolution on the order of the laser pulse width $\Delta t \sim 150$ fs [11]. After mixing, the sum-frequency photons are detected by a cooled photomultiplier tube equipped with a monochromator for additional energy resolution. Furthermore, a streak camera with $\Delta t \sim 10$ ps is used in experiments which required relatively less time resolution than that obtained using the sum-frequency method.

Figure 1(b) displays the field-dependent photoluminescence (PL) from a SSL with 9% Mn, excited by a linearly polarized beam at $E=2.945$ eV, which creates equal populations of spin-up and spin-down carriers. This time-integrated, polarization-resolved σ^+ component of the heavy hole PL from the $Zn_{1-x}Mn_xSe$ layers results from the recombination of a spin $J=-\frac{3}{2}$ hole with a spin $S=-\frac{1}{2}$ conduction electron in the magnetic quantum well. The confining potential deepens for this exciton state with increasing magnetic field, and the corresponding change in the ground state is seen as a decrease in the PL peak energy [Fig. 1(c)]. This is accompanied by an increase in PL intensity due to larger electron-hole correlations with stronger localization. The tunability of the confining potential results from a Zeeman splitting via an exchange interaction between the charge carriers and the Mn^{2+} ions [12]. This splitting produces a field-tunable spin-dependent confining potential and net polarization $P=(\sigma^+-\sigma^-)/(\sigma^++\sigma^-)$ [inset, Fig. 1(b)]. While the σ^+ PL peak shifts to lower energy, the σ^- PL peak energy moves to higher energy with increasing field since it originates from carriers whose spin is opposed to the applied field. Thus for $B<0.5$ T the quantum well potential depth for this spin state decreases with increasing field resulting in a larger excitonic Bohr radius and a decrease in the observed σ^- PL intensity. For $B\sim0.5$ T, where the SSL is formed, the σ^- component has decreased dramatically and is now indistinguishable from the ZnSe buffer layer PL [13]. Unlike PL in SSL's with strain in *both* magnetic and nonmagnetic layers [8], no σ^- PL from the SSL was observed at higher fields which has implications for spin scattering in the nonmagnetic layers. Measurements on other SSL's in the series showed qualitatively similar behavior [11], so from here on we will focus on a sample with $x=0.09$.

A series of field-dependent time-resolved measurements were performed to directly probe the physical processes that underlie the steady-state data. Figure 2(a) shows streak camera measurements taken at the peak of the σ^+ component of the PL for several values of the magnetic field. For $B<0.5$ T, data are obtained for the σ^- PL component in a similar manner. These data confirm the field-dependent increase in PL efficiency found in the time-integrated data and also show an increase in τ^+, the PL lifetime of σ^+. This unexpected increase may be attributed to a decrease in nonradiative decay from scattering of the excitons due to impurities or disorder at the interfaces [4] as the spin down carriers become more localized in the field-induced $Zn_{1-x}Mn_xSe$ "wells." This decrease in scattering also contributes to the enhanced radiative recombination that is manifested in higher PL intensity. Figure 2(b) also shows the field dependence of τ^- which is the radiative lifetime for the σ^- PL component. A dramatic decrease of τ^- is observed in the vicinity of $B\sim0.5$ T where the SSL formation occurs. The decrease coincides with the spatial separation of carriers in the SSL and their fast relaxation into the magnetic

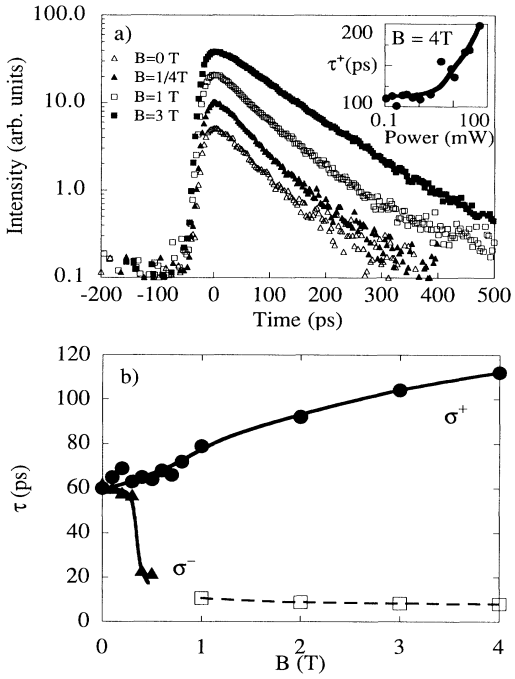

FIG. 2. (a) Time-resolved σ^+ PL from the sample of Fig. 1 at $T=4.2$ K. Inset: σ^+ PL lifetime versus excitation power at $B=4$ T. (b) σ^+ and σ^- PL lifetimes with applied magnetic field from single exponential fits of (a). Open squares represent PL from the ZnSe buffer layer.

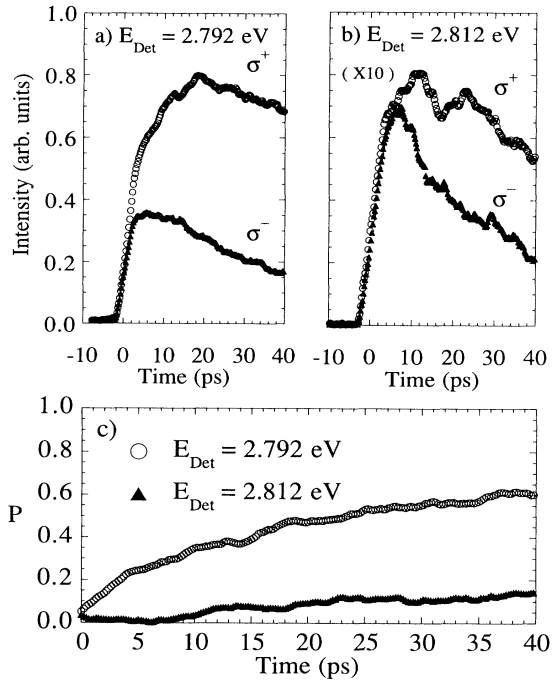

FIG. 3. Time- and polarization-resolved PL before spatial separation of the distinct spin states from the sample of Fig. 1 at $B=\frac{1}{4}$ T for detection energies (a) at the ground state, and (b) 20 meV above the ground state. (c) The resulting time-dependent polarization.

quantum wells before recombination via the spin-up (σ^-) state. This results in the field-dependent polarization of Fig. 1. The data are accumulated under low excitation density (<1 mW) where the PL lifetimes are nearly independent of excitation power and energy in the regime of interest [inset, Fig. 2(a)]. At carrier densities $>10^{10}$ cm^{-2} the exciton lifetime increases due to electron-electron scattering and resulting nonthermalized carrier populations [14]. Although the static PL linewidths do not vary with excitation power or magnetic field, the dynamical results are extremely sensitive to both. The present work indicates that traditional static polarization data (Fig. 1) result from changes in *both* the intensities and lifetimes of σ^+ and σ^-—a characteristic that is not typically considered in theoretical interpretations of PL polarization [2].

A remarkable change in exciton dynamics is observed upon formation of the SSL and is more clearly resolved by femtosecond upconversion spectroscopy. For $B<0.5$ T the SSL has not formed, and the PL for both σ^+ and σ^- originates from the magnetic $Zn_{1-x}Mn_xSe$ quantum well layers. The spin polarization of photoexcited carriers during cooling to the exciton ground state can be directly probed by varying the *detection* energy of the PL. Since detection energies above the time-integrated PL peak probe the carriers which have radiatively recombined before reaching the exciton ground state, the time-dependent polarization monitored at these higher energies provide a snapshot of spin relaxation as the carriers cool. Figure 3 shows the time-dependent polarization-resolved PL intensity for detection near the exciton ground state [Fig. 3(a)] and several time-integrated PL linewidths higher in energy [Fig. 3(b)]. Since the carriers are less likely to radiatively recombine in the excited state, the signal intensity for both PL components at higher energies is much less than at lower energies. Figure 3(c) displays the time-dependent polarization at the two detection energies, revealing a spin scattering time of order tens of picoseconds. Contrary to experimental and theoretical expectations [3] which suggest that exciton scattering in DMS quantum wells is almost instantaneous and dominated by nonmagnetic electron-hole correlations in low dimensional systems, these data are consistent with predictions of spin scattering in magnetic heterostructures due to *sp-d* exchange interactions [2]. Accordingly, the scattering times increase with decreasing x [11].

In Fig. 4, the onset of the σ^+ PL is presented for $B>B_{SSL}$ with the detection energy set to the peak of the luminescence intensity. These data show the nonequilibrium relaxation of excitons into the ground state as the quantum well depth within the SSL is varied in a single sample. The curves may be normalized by their respective fields to show that the carrier cooling is independent of confining potential [11]. For fields $B>0.5$ T where

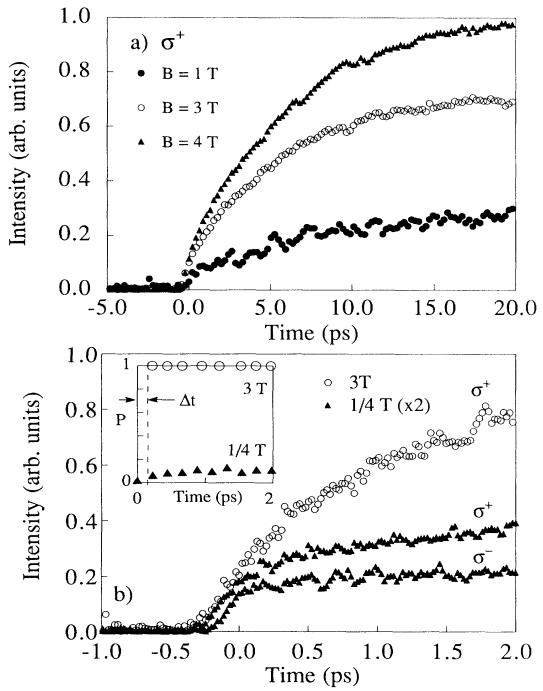

FIG. 4. (a) Time- and polarization-resolved PL with the spin states spatially separated. (b) The initial 2 ps of the luminescence in (a) and the net polarization (inset).

the SSL has formed and the spin states for the σ^- are localized in the ZnSe layers, no σ^- PL from the SSL is detected at any time. Therefore, in contrast to the dynamics in lower fields, the resulting polarization is instantaneous [inset, Fig. 4(b)]. As the system is excited with linearly polarized light, this indicates an extremely rapid spin-flip relaxation of carriers from the nonmagnetic layers into the magnetic quantum wells on a time scale much shorter than the exciton lifetime. Since the heavy and light holes are degenerate in the ZnSe layers, mixing of the hole states may play an important role in this spin relaxation process [2]. The ultrafast temporal behavior of the PL is qualitatively similar to that seen in other DMS [3] as well as high quality $GaAs/Al_xGa_{1-x}As$ heterostructures [15]. As shown in Fig. 4(b), in all fields and in both polarizations, there is an extremely fast rise in the PL intensity which develops over time scales shorter than the time resolution of the experiment (< 150 fs). This indicates that excitons capable of radiatively recombining, i.e., those with center of mass momentum $K=0$ and those with energy within a homogeneous linewidth of $K=0$, form instantaneously. Finally, a distinct difference appears between the two polarizations for times > 200 fs. In all fields, the σ^+ intensity slowly increases and reaches a maximum as hot carriers cool to states which can radiatively recombine [14,15]. However, at low fields the σ^- PL shows almost no increase after the initial rise. This disparity supports the previous observation (Fig. 3) of concurrent spin-flip and energy relaxation of the carriers.

In summary we have directly measured the spin-dependent dynamics of excitons in DMS spin superlattice structures using femtosecond polarization-resolved upconversion spectroscopy. Despite expectations for ultrafast nonmagnetic spin scattering in heterostructures, this class of systems demonstrates the ability to explore magnetic interactions in quantum confined geometries.

We thank J. J. Baumberg for critical readings of the manuscript. This work was supported by NSF Grants No. DMR 92-07567 and No. DMR 92-08400, and the IBM Corporation.

[1] S. Schmitt-Rink, D. S. Chemla, and D. A. B. Miller, Adv. Phys. **38**, 89 (1989).
[2] T. Uenoyma and L. J. Sham, Phys. Rev. Lett. **64**, 3070 (1990); G. Bastard and L. L. Chang, Phys. Rev. B **41**, 7899 (1990); G. Bastard and R. Ferreira, Surf. Sci. **267**, 335 (1992).
[3] M. R. Freeman *et al.*, Phys. Rev. Lett. **64**, 2430 (1990).
[4] M. Kohl *et al.*, Phys. Rev. B **44**, 5923 (1991); P. Roussignol *et al.*, Surf. Sci. **267**, 360 (1992).
[5] S. Bar-ad and I. Bar-Joseph, Phys. Rev. Lett. **68**, 349 (1992).
[6] N. Dai *et al.*, Phys. Rev. Lett. **67**, 3824 (1991).
[7] W. C. Chou *et al.*, Phys. Rev. Lett. **67**, 3820 (1991).
[8] W. C. Chou *et al.*, Phys. Rev. B **46**, 4316 (1992).
[9] M. von Ortenberg, Phys. Rev. Lett. **49**, 1041 (1982).
[10] H. Mahr and M. D. Hirsch, Opt. Commun. **13**, 96 (1975); J. Shah, IEEE J. Quantum Electron. **24**, 276 (1988).
[11] J. F. Smyth *et al.* (to be published).
[12] *Diluted Magnetic Semiconductors,* edited by J. K. Furdyna and J. Kossut, Semiconductors and Semimetals (Academic, San Diego, 1988), Vol. 25.
[13] The origin of this ancillary PL was confirmed by measurements on a 1 μm thick ZnSe epilayer. Although the PL from the buffer layer is unpolarized, at higher fields its σ^+ component is completely masked by the strong σ^+ in the SSL.
[14] G. Bastard, *Wave Mechanics Applied to Semiconductor Heterostructures* (Les Editions de Physique, Paris, France, 1988).
[15] T. C. Damen *et al.*, Phys. Rev. B **42**, 7434 (1990).